J Biol Inorg Chem (2017) 22:673–683
DOI 10.1007/s00775-017-1452-5

ORIGINAL PAPER

Functional disruption of peroxiredoxin by bismuth antiulcer drugs attenuates *Helicobacter pylori* survival

Yuen-Yan Chang[1] · Tianfan Cheng[1,2] · Xinming Yang[1] · Lijian Jin[2] · Hongzhe Sun[1] · Hongyan Li[1]

Received: 20 February 2017 / Accepted: 21 March 2017 / Published online: 30 March 2017

Abstract Bismuth drugs have been used clinically to treat infections from *Helicobacter pylori,* a pathogen that is strongly related to gastrointestinal diseases even stomach cancer. Despite extensive studies, the mechanisms of action of bismuth drugs are not fully understood. Alkyl hydroperoxide reductase subunit C (AhpC) is the most abundant 2-cysteine peroxiredoxin, crucial for *H. pylori* survival in the host by defense of oxidative stress. Herein we show that a Bi(III) antiulcer drug (CBS) binds to the highly conserved cysteine residues (Cys49 and Cys169) with a dissociation constant (K_d) of Bi(III) to AhpC of 3.0 (±1.0) × 10^{-24} M. Significantly the interaction of CBS with AhpC disrupts the peroxiredoxin and chaperone activities of the enzyme both in vitro and in bacterial cells, leading to attenuated bacterial survival. Moreover, using a home-made fluorescent probe, we demonstrate that Bi(III) also perturbs AhpC relocation between the cytoplasm and membrane region in decomposing the exogenous ROS. Our study suggests that disruption of redox homeostasis by bismuth drugs via interaction with key enzymes such as AhpC contributes to their antimicrobial activity.

Keywords Bismuth drug · Enzyme · Oxidative stress · Peroxiredoxin · Molecular mechanism

Introduction

Antimicrobial resistance is on the rise which posts huge threats on public health. Re-use of antimicrobial metal ions, e.g., Ag^+ and Bi^{3+} has received renewed attention due to their potentials in killing multidrug-resistant bacteria [1] and in improving the cure rates of infections from resistant strains [2]. Bismuth drugs including colloidal bismuth subcitrate (CBS) and ranitidine bismuth citrate (RBC) have been widely used clinically to treat gastrointestinal disorder and *Helicobacter pylori* infection [3]. *H. pylori*, a Gram-negative bacterium, is closely associated with gastrointestinal diseases including gastritis, peptic ulcer, and even gastric cancer [4–7]. Combination of bismuth drugs with antibiotics either as triple or quadruple therapies have been suggested as the first-line therapy and importantly exhibit excellent success rates in eradiation of *H. pylori* even for antibiotic resistance strains [8–10]. Despite being used clinically for over decades, the mechanism of action of bismuth drugs still remains elusive. Much attention has been previously devoted to understanding how bismuth interferes with nickel homeostasis [5, 11–15], owing to the importance of nickel-containing enzymes, e.g., urease and [Ni, Fe] hydrogenase for its survival and pathogenesis. Recent metalloproteomics studies reveal that the identified bismuth-binding proteins are involved in multiple biological pathways [16, 17], indicative of multi-targeted mechanism of action of the drugs.

Defense of oxidative stress is crucial for *H. pylori* survival in the host as bacterial infection could induce inflammatory response, resulting in oxidative burst, which

Electronic supplementary material The online version of this article (doi:10.1007/s00775-017-1452-5) contains supplementary material, which is available to authorized users.

✉ Hongzhe Sun
hsun@hku.hk

✉ Hongyan Li
hylichem@hku.hk

[1] Department of Chemistry, The University of Hong Kong, Pokfulam Road, Hong Kong SAR, People's Republic of China

[2] Faculty of Dentistry, The University of Hong Kong, Sai Ying Pun, Hong Kong, People's Republic of China

accumulates in the stomach and rapidly eliminates the bacterium if without a comprehensive defensive system. Deficiency in the defensive system of *H. pylori* could finally lead to substantial impairment of the bacterial viability and colonization [18]. To counter oxidative stress, *H. pylori* has developed a range of methods including expression of antioxidant enzymes such as superoxide dismutase (SOD), catalase (Kat) and alkyl hydroperoxide reductase subunit C (AhpC) [18]. AhpC, sometimes also called the thiol-specific antioxidant (TsaA), from *H. pylori* is a member of ubiquitous 2-cysteine peroxiredoxins family with a molecular weight of 26 kDa, and protects *H. pylori* from oxidative damages originated from hydrogen peroxide (H_2O_2), peroxynitrite and a wide range of organic hydroperoxides through peroxidase activity [19, 20]. It is highly expressed as the most abundant antioxidant protein for decomposing H_2O_2 and organic peroxides and is essential for the survival and growth of *H. pylori* [21, 22]. A high expression level of AhpC is noted in *H. pylori* isolated from gastric cancer patients [23]. Like those yeast and human peroxiredoxins, *H. pylori* AhpC can also act as a molecular chaperone for prevention of protein misfolding as well as assisting the refolding of denatured proteins under oxidative stress [20, 24, 25].

We have previously mined the putative protein targets of bismuth drugs by various metalloproteomic approaches [16, 17, 26]. AhpC was identified as one of the bismuth-binding proteins in *H. pylori* [26]. Herein, we carried out detailed in vitro and in vivo studies on the interaction of a bismuth drug (CBS) with AhpC and evaluated the biological consequence of such an interaction. We show that Bi(III) binds to the conserved cysteine residues, and in vitro study reveals that binding of Bi(III) disrupts both peroxidase and chaperon activity of AhpC. Furthermore, inhibition of AhpC activity by Bi(III) attenuated bacterial growth under oxidative stress. Using home-made fluorescent probe, bismuth perturbation of stress-induced protein translocation of AhpC is also observed. The study indicates that AhpC serves as an important target of bismuth drugs.

Materials and methods

Construction of expression plasmids

The *ahpC* gene was amplified from *H. pylori* 26695 genomic DNA by polymerase chain reaction (PCR) using KOD DNA polymerase and the primer pair AhpC_F/AhpC_R as shown in Table S1. PCR product was purified using Illustra GFX PCR DNA and Gel Band Purification Kit (GE Healthcare). After digestion by corresponding restriction endonucleases (New England Biolabs), the fragment of *ahpC* was ligated into pET-28a vector to obtain the plasmid pET-AhpC. Plasmids pET-AhpC-C49A and pET-AhpC-C169A were generated by Phusion Site-Directed Mutagenesis Kit (New England Biolabs) using primer pairs AhpC_C49A_F/AhpC_C169A_R and AhpC_C169A_F/AhpC_C169A_R, respectively, while pET-AhpC served as the template. The primer pair AhpC_C49A_F/AhpC_C49A_R was used for constructing the plasmid pET-AhpC-C49C169A, using pET-AhpC-C169A as the template.

Protein expression and purification

Plasmid pET-AhpC (and pET-AhpC-C49A and pET-AhpC-C169A and pET-AhpC-C49C169A) were transformed into *E. coli* BL21(DE3). The overnight culture was 1:100 subcultured into fresh LB medium in the presence of 50 μg/mL kanamycin. Bacteria were grown at 37 °C until OD600 was about 0.6. Protein expression was induced at 25 °C overnight using 0.2 mM IPTG. Bacteria were harvested by centrifugation at 4000*g* for 30 min at 4 °C and were resuspended in 20 mM Tris–HCl, pH 7.4, 300 mM NaCl containing 20 mM imidazole supplemented with 1 mM PMSF.

Cells were lysed by sonication, after which the lysate was centrifuged at 4 °C at 10,000*g* for 30 min and was applied to HisTrap HP column (GE Healthcare) pre-equilibrated with the same Tris buffer. Tris buffers containing 20 and 50 mM imidazole were used to remove weakly bound impurities while Tris buffer with 300 mM imidazole was used for elution. Fractions were collected and subjected to analysis by 12% sodium dodecyl sulfate–polyacrylamide gel electrophoresis (SDS-PAGE). The peak fraction was buffer exchanged with 20 mM Tris–HCl, pH 7.6, 120 mM NaCl for thrombin cleavage of His-tag on AhpC and its variants. Thrombin cleavage was carried out at 16 °C for an overnight and the cleavage product was purified by HisTrap HP column and then subjected to further purification by HiLoad 16/60 Superdex 200 prep grade (GE Healthcare) using 20 mM Tris–HCl, pH 7.4, 300 mM NaCl. The peak fractions were pooled and concentrated by Amicon Ultra-15 centrifugal filter unit (Millipore). BCA Protein Assay Kit (Novagen) was used to determine the protein concentration and MALDI-TOF MS was used to validate the identity of the purified protein.

Interaction between Bi(III) and AhpC and its mutants by UV–Vis Spectroscopy

Bi(III) binding to AhpC and its mutants were monitored by UV–Vis spectroscopy, using a 1-cm pathlength quartz cuvette on Cary 50 UV–Vis spectrometer at room temperature. UV spectra were collected from 600 to 200 nm at a speed of 240 nm/min. AhpC and its mutants were pre-reduced by TCEP and were freshly prepared in HEPES buffer (10 mM HEPES, pH 7.4, 100 mM NaCl, 400 μM

TCEP). HEPES buffer was also used for baseline correction while Bi(NTA) served as the Bi(III) source. 0.1–2.0 molar equivalents of Bi(III) were titrated into protein samples and UV spectra were recorded after 10-min incubation at room temperature. Changes in absorbance at 360 nm were plotted and the dissociation constant (K_d) was determined by non-linear curve fitting using Ryan–Weber equation [27]:

$$\Delta F = C\frac{([P]+[M]+K_d)-\sqrt{([P]+[M]+K_d)^2-4[P][M]}}{2}$$

where ΔF is the change in signals (absorbance), C is the parameter for the change in signals per unit complex, $[P]$ refers to the protein concentration, and $[M]$ is the concentration of metal ions.

Analysis of oligomerization state

Analytical Tricorn Superdex 75 10/300 GL column (GE Healthcare) was used to examine the oligomerization state of AhpC and Bi-bound AhpC. The column was calibrated with Gel Filtration Calibration Kit—Low Molecular Weight (GE Healthcare) prior to analysis. AhpC (50 μM) was prepared in HEPES buffer [10 mM HEPES, 100 mM NaCl, pH 7.4] while the Bi-bound AhpC was prepared by incubating AhpC (50 μM) with Bi(III) (up to 2 molar equivalents) for 2 h at 37 °C. The column was equilibrated with the same HEPES buffer and analysis was performed at 4 °C at a flow rate of 0.5 mL/min with a detector to monitor the absorbance at 280 nm.

Evaluation of ROS level by FOX assay

FOX assay was performed using hydrogen peroxide (H_2O_2), *tert*-butyl hydroperoxide (*t*-BuOOH) and cumene hydroperoxide ($PhC(CH_3)_2OOH$) to evaluate the peroxiredoxin activity of AhpC and its mutants according to a previously reported protocol with some modifications [28]. In brief, each assay mixture consists of AhpC (or its mutants) (pre-reduced by excess tris(2-carboxyethyl) phosphine, (TCEP), 2.0 μM in H_2O_2 reaction or 2.5 μM in *t*-BuOOH and $PhC(CH_3)_2OOH$), different ROS species (H_2O_2, *t*-BuOOH or $PhC(CH_3)_2OOH$; 0–200 μM) in PBS buffer in the presence of DTT (100 μM) for evaluating the multiple turnover efficiency of AhpC. To evaluate the effect of Bi(III) on the peroxiredoxin activity of AhpC and its mutants, AhpC (or its mutants) (pre-reduced with TCEP) was incubated with CBS (5 molar equivalents) at 37 °C for 15 min prior to FOX assay.

FOX working reagent was prepared by mixing FOX reagent A (25 mM ferrous ammonium sulfate in 2.5 M H_2SO_4) and FOX reagent B (100 mM D-sorbitol, 125 μM xylenol orange in ddH_2O) in 1:100. Reaction was carried out at 37 °C and quenched by transferring the reaction mixture (10 μL) to FOX working reagent (200 μL) in 96-well plate at different time intervals. Samples were then incubated at room temperature for at least 30 min prior to the record of the absorbance at 570 nm. The concentration of ROS species was estimated from the standard calibration curves of the three ROS species. The results of triplicates were averaged and the activities of Bi(III)-treated AhpC and its mutants were normalized against that of the samples without incubation with Bi(III) ions for each ROS species individually.

To study the effect of Bi(III) on the enzyme kinetics of AhpC, the reaction rate of AhpC with or without incubation with CBS was measured at 1-min interval in the presence of varying concentrations of the three ROS species ranging from 0 to 200 μM. The reaction rates were plotted against the concentrations of ROS species added, the parameters of enzyme kinetic (Michaelis constant, K_m; turnover number, k_{cat} and catalytic efficiency, k_{cat}/K_m) were determined from the non-linear curve fitting using Michaelis–Menten equation in GraphPad Prism.

To understand the effect of antimicrobial on the oxidative defense of bacteria, *H. pylori* strain 26695 and clinical isolate A30651 were cultured (with and without the supplement of 10 or 20 μg/mL CBS) and were harvested. Cell lysate was obtained by sonication and FOX assay was performed using *tert*-butyl hydroperoxide (*t*-BuOOH) as the ROS substrate.

Refolding and reactivation of denatured citrate synthase by AhpC

Chaperonin-assisted refolding of citrate synthase was used to analyze the effect of Bi(III) on the chaperone activity of AhpC. Citrate synthase refolding and reactivation assay was performed according to previous reports [29, 30]. In brief, citrate synthase (as 3.2 M $(NH_4)_2SO_4$ suspension, pH 7.0 upon received) was first prepared according to the recommended protocol of the manufacturer (Sigma). It was then denatured in denaturing buffer (20 mM potassium phosphate, pH 7.4, 6 M guanidine hydrochloride, 3 mM DTT, 2 mM EDTA) at room temperature for 90 min. The concentration of denatured citrate synthase was determined by monitoring UV absorption at 280 nm with extinction coefficient of citrate synthase of 8900 M^{-1} cm^{-1}.

AhpC (100 μM) was pre-treated with 10 mM H_2O_2 at 37 °C for overnight with or without the addition of CBS (1, 2 or 5 molar equivalents) at 37 °C for an hour. Renaturation of citrate synthase was performed by the addition of denatured citrate synthase to refolding reaction mixture (10 mM $MgCl_2$ and 1 mM oxaloacetic acid in 20 mM potassium phosphate, pH 7.4) in the presence of equimolar amounts of H_2O_2-treated AhpC or Bi-bound AhpC. AhpC-dependent citrate synthase refolding assay was carried out at 37 °C

and the absorbance at 500 nm was monitored on Varioskan Flash Multimode Reader (Thermo Fisher) until the curve reached a plateau.

Activities of the renatured citrate synthase were assessed by its catalytic efficiency on the condensation reaction of acetyl-CoA and oxaloacetic acid. The enzymatic assay was initiated by adding 40 μL of refolding mixture to the reaction buffer consisting of 400 μM oxaloacetic acid, 160 μM acetyl-CoA in 20 mM potassium phosphate, pH 7.4. The assay was performed at room temperature and the absorbance at 233 nm, owing to the disappearance of acetyl-CoA, was recorded on Varioskan Flash Multimode Reader (Thermo Fisher) until the curve reached a plateau. The effect of Bi(III) on the chaperone activity of AhpC was normalized against the activity of the bismuth-untreated AhpC. The enzymatic activity of the denatured citrate synthase in the absence of AhpC (or spontaneous refolding) was used as the negative control.

Evaluation of tolerance towards oxidative stress by AhpC in *E. coli*

To understand the effect of Bi(III) on the antioxidant activity of AhpC in the bacterium, overnight cultures of *E. coli* wild-type K12 strain BW 25113 (WT) [31] and its *ahpC* knockout strain JW0598 from KEIO collection (KO) [32] were prepared in LB medium. The overnight cultures of the two strains were washed in M9 minimal medium for three times and were treated with CBS (50 μM) in M9 minimal medium at 37 °C for 4 h. The OD_{600} of the cultures was then adjusted to 0.1–0.2 using fresh M9 minimal medium (with or without the supplement of 50 μM CBS). Bacterial cultures were incubated with various concentrations of *tert*-butyl hydroperoxide (*t*-BuOOH, 0, 0.5, 1, 2, 5 mM) at 37 °C for 30 min. Cells were washed with M9 minimal medium and were resuspended in fresh M9 minimal medium for growth at 37 °C for 20 h, after which the cell densities were recorded. The growth of wild type (WT), Bi(III)-treated wild type (WT + Bi) and *ahpC* knock-out strains (KO) at different concentrations of *t*-BuOOH was normalized against that of the corresponding samples with *t*-BuOOH treatment.

For analysis of growth rate of the bacterium when subjected to oxidative stress (in the absence or presence of CBS), CBS (50 μM) was supplemented (in M9 minimal medium) to the culture of the WT and KO strains at 37 °C for 4 h, whose OD_{600} were then adjusted to be 0.1–0.2 with fresh M9 minimal medium (with or without the supplement of 50 μM CBS). *t*-BuOOH (5 mM) was added to culture medium and cells were treated for 30 min at 37 °C, then washed and resuspended in fresh M9 minimal medium for growth at 37 °C. Cell densities at different time intervals (0, 2, 6, 10, 20 h) were measured to evaluate the effect of Bi(III) ions on the bacterial growth under oxidative stress.

Helicobacter pylori culture

Helicobacter pylori strain 26695 and a clinical isolate strain A30651 were cultured on Columbia agar base in the presence of 7% laked horse blood (Oxoid) and *H. pylori* selective supplement Dent (Oxoid) at 37 °C under microaerobic condition using Campygen 2.5L (Oxoid) for 3 days. The bacteria were then inoculated to Brucella broth with 1.4% β-cyclodextrin at 37 °C with agitation for an overnight without or with the supplement of CBS (10 or 20 μg/mL). To prepare the cell lysate, cells were harvested and washed with PBS (pH 7.4) for three times and then lysed by sonication.

Allelic exchange for mutagenesis in *H. pylori*

To perform nonpolar gene knock-out in *H. pylori*, a plasmid pBS-NP-AphA3(-) was constructed. The nonpolar kanamycin resistance gene (*aphA3*) was designed as described previously [33], i.e., *aphA-3* was preceded by translation stop codons in all three reading frames (underlined) and was immediately followed by a consensus ribosome-binding site, GGAGG, and a start codon (double-underlined). Two SmaI sites are located at the two ends.

CCCGGGTGACTAACTAGGAGGAATAAATG
aphA-3 TAGTACCTGGAGGGAATAATGACCCGGG

The nonpolar *aphA-3* gene cassette was amplified from the plasmid pTM117 [34] using the following two primers:

aphA-3-NP-for: 5′-TCCCCCGGGTGACTAACTAGGAGGAATAAATGGCTAAAATGAGA-3′
aphA-3-NP-rev: 5′-TCCCCCGGGTCATTATTCCCTCCAGGTACTAAAACAATTCATC-3′

The generated fragment was digested by SmaI and ligated in pBlueScript II SK(+), generating pBS-NP-AphA3(-). Two DNA fragments (550 bp) flanking the *ahpC* gene (named as "Up" or "Down", respectively) were amplified from *H. pylori* 26695 strain genome DNA by the following primer pairs (the stated enzyme sites):

dAhpC-Up-For (XbaI): GGGGGTCTAGA GATCACTGCTCATGGATTTAA
dAhpC-Up-Rev (BamHI): GGGGGGATCC ATCGTAACTCCTTAAGTGTTTT
dAhpC-Down-For (EcoRI): GGGGGGAATTC TCGGCTTAATTCTTTTAACCAA

dAhpC-Down-Rev (KpnI): GGGGGGTACC TAAAATC TTAAAGGCTCCACATG

The DNA fragments were inserted into the up- and down-stream of the nonpolar *aphA-3* gene cassette in pBS-NP-AphA3(-), respectively, generating the nonpolar mutagenesis plasmid pBS-NP-AphA3(-)-dAhpC. The in vivo knock-out mutagenesis was achieved by standard homologous recombination for *H. pylori* [35].

Confocal imaging of AhpC-overexpressing *E. coli*

To monitor the cellular localization of AhpC in AhpC-overexpressing *E. coli* upon different treatment (in the presence of CBS or excess ROS or both), Ni–*NTA-AC* was applied to track the intracellular AhpC (encoded with a His-tag) in *E. coli* cells according to previous reports with some modifications [36, 37]. Overexpression of His-tagged AhpC in *E. coli* BL21(DE3) was done as described in the previous section, with or without addition of CBS (50 μM) during protein expression. Then a representative of ROS, e.g., *t*-BuOOH (2 mM) was added to the bacterial culture at 37 °C for 5 h, after which the cells were collected by centrifugation, followed by washing with PBS buffer (pH 7.4) for three times. The cell pellet was resuspended in PBS buffer and was incubated with Ni-*NTA-AC* (100 μM) at 37 °C for 30 min. Cells were washed with PBS buffer for three times prior to fixation using 4% paraformaldehyde in PBS buffer at room condition for 15 min. Fixation was quenched by removal of paraformaldehyde by centrifugation and the cells were washed with PBS buffer thoroughly for three times. For staining the cell membrane of the bacteria, cells were incubated with BODIPY 558/568® C12 (Life Technologies) at room condition for 15 min, followed by washing with PBS buffer for three times. OD_{600} of the bacterial samples was adjusted to 0.2–0.3 by PBS prior to analysis by Carl Zeiss LSM700 inverted confocal microscopy with 63× 1.40NA oil objective and excitation with the 405 nm laser for Ni-*NTA-AC* and the 555 nm laser for the lipid probe BODIPY® stain.

Results and discussion

In vitro characterization of bismuth binding to AhpC

AhpC was overexpressed and purified as described in the experimental section. The interaction of Bi(III) with recombinant AhpC was monitored by UV–Vis spectroscopy. Upon titration of up to 80 μM of Bi(NTA) to 40 μM of AhpC solution in 10 mM HEPES containing 100 mM NaCl, 400 μM TCEP at pH 7.4, an absorption band centered at ca. 350 nm appeared (Fig. 1a), increased in its intensity and leveled off at a molar ratio of [Bi(NTA)]/[AhpC] of ca. 0.5, indicating that each AhpC dimer binds one Bi(III) (Fig. 1b). The absorption at 350 nm is assignable to π(S)(Cys) → Bi(III) ligand-to-metal charge transfer transition [38], suggesting that cysteine residues of AhpC are involved in the binding. The binding affinity of Bi(III) to AhpC was determined by fitting the UV titration curve to the Ryan–Weber equation as previously reported [12], giving rise to a dissociation constant of Bi(NTA) to the protein of 1.1 ± 0.3 μM. By taking into account the binding constant of Bi(NTA) (log $K_a = 17.55$) [27], the dissociation constant (K_d) of Bi(III) to AhpC was calculated to be 3.0(±1.0) × 10^{-24} M. Such a high affinity of Bi(III) towards thiolate has been seen previously [13, 39].

AhpC possesses two cysteine residues in the active site with different reactivity towards the enzyme substrates, ROS [19]. To examine whether the cysteine residues possess asymmetric reactivity towards Bi(III), a single or double point mutation of cysteine residues to alanine (C49A and C169A) were carried out by site-directed mutagenesis. As shown in Fig. 1b and S1A-B, similar UV absorbance

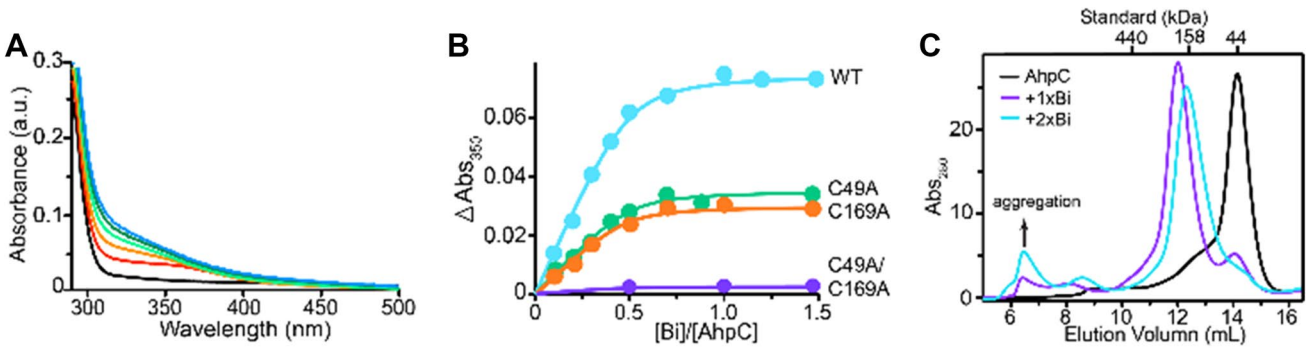

Fig. 1 Binding of Bi(III) to recombinant AhpC. **a** UV–Vis spectra of AhpC (40 μM) with addition of different molar equivalents of Bi(NTA). **b** Changes of UV absorbance at 350 nm vs molar ratios of [Bi]/[protein] for the wild-type AhpC and its variants. **c** Gel filtration profiles of AhpC (40 μM) pre-treated with TCEP without and with addition of 1 and 2 molar equivalents of CBS

changes at 350 nm with the molar ratios of [Bi(NTA)]/[protein] were observed when Bi(III) was titrated to AhpC-C49A or AhpC-C169A, and the binding stoichiometries of Bi(III) to both AhpC-C49A and AhpC-C169A were identical to that of the wild-type AhpC although only half of absorbance changes at 350 nm were observed. In contrast, negligible increases in UV absorbance at 350 nm were observed for AhpC-C49C169A (Fig. 1b and S1C) under identical conditions, suggesting that both Cys49 and Cys169 of AhpC were involved in the binding of Bi(III) without substantial difference in their reactivity.

Subsequently, the oligomerization states of AhpC upon Bi(III) binding was analyzed by analytical gel filtration chromatography. In the presence of excess amounts of tris(2-carboxyethyl)phosphine (TCEP), AhpC was eluted as a major peak at 14.4 mL, corresponding to the molecular weight of ca. 44 kDa, indicating that AhpC exists predominately as a dimer (Fig. 1c). Upon the addition of one molar equivalent of Bi(III), a new peak appeared at ~12.1 mL, corresponding to a high oligomeric state of the protein, accompanied by significant decrease in the intensity of the peak at 14.4 mL. Incubation of two molar equivalents of Bi(III) led to almost completely disappearance of the protein dimeric peak, indicative of the presence of multimeric AhpC upon Bi(III) binding (Fig. 1c).

Bi(III) drug inhibits antioxidant activity of AhpC

AhpC can react with various ROS, including hydrogen peroxide and organic hydroperoxide [40]. To investigate the effects of Bi(III) binding on peroxiredoxin activity of AhpC, FOX assay [28] was used in the presence of simple oxidant hydrogen peroxide (H_2O_2), *tert*-butyl hydroperoxide (*t*-BuOOH) and cumene hydroperoxide ($PhC(CH_3)_2OOH$), which represents the class of lipid hydroperoxides. AhpC (pre-reduced by excess amounts of TCEP) was incubated with five molar equivalents of CBS prior to its reaction with different ROSs. Upon addition of 0–200 μM of ROS, peroxiredoxin activity of AhpC exhibited an evident drop against all of the ROSs studied (Fig. 2a–c). Based on the normalized activity, it is noted that treatment of CBS led to the antioxidant activities of AhpC decreased by roughly 50–70%, with statistical significance (Figure S2A). The kinetics properties of AhpC without or with treatment of Bi(III) towards reacting with H_2O_2, *t*-BuOOH and $PhC(CH_3)_2OOH$ including Michaelis

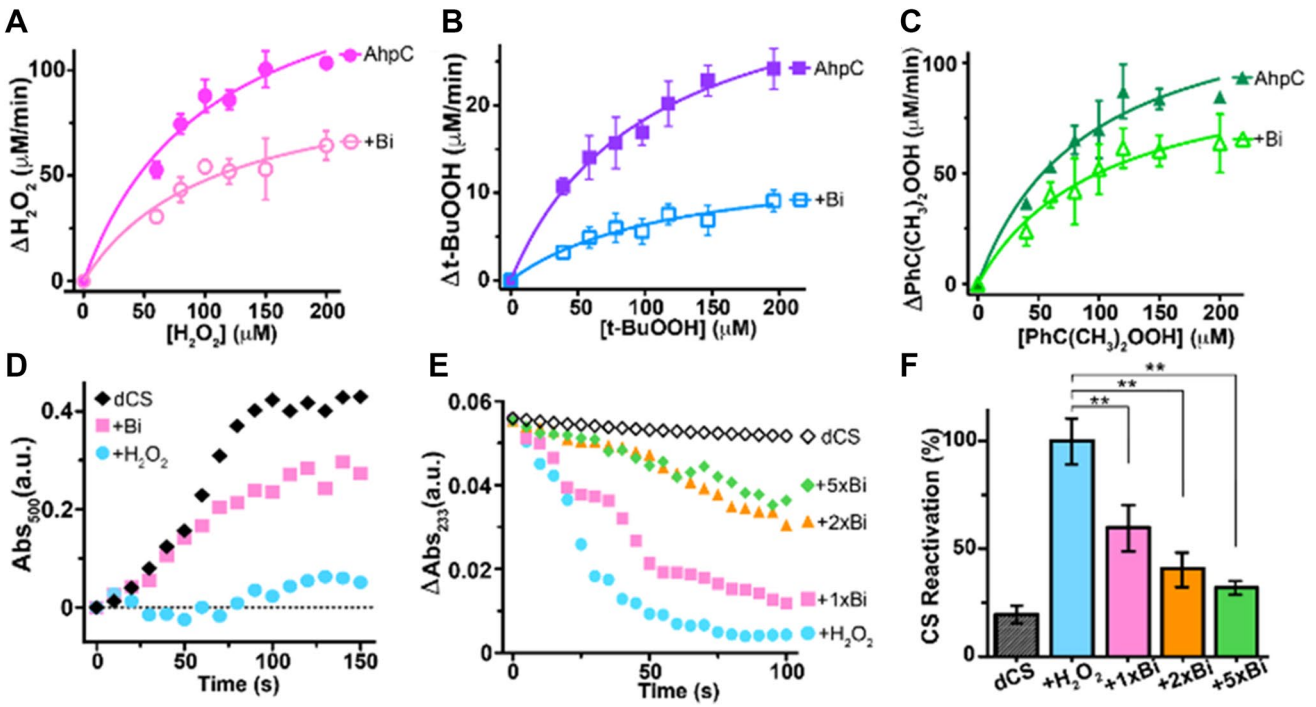

Fig. 2 Analysis of enzymatic activity of AhpC by FOX assay. Antioxidant activity of AhpC and CBS-treated AhpC towards **a** H_2O_2, **b** *tert*-butyl hydroperoxide (*t*-BuOOH) and **c** cumene hydroperoxide ($PhC(CH_3)_2OOH$) in the presence of DTT. Chaperone activity of AhpC was evaluated by the refolding and reactivation of citrate synthase. **d** Time-dependent UV absorbance at 500 nm of denatured citrate synthase alone (dCS) and in the presence of H_2O_2-treated AhpC or Bi-AhpC. **e** Time-dependent UV absorbance at 233 nm for the decomposition of substrate acetyl-CoA by denatured citrate synthase alone (dCS), H_2O_2-treated AhpC in the absence ($+H_2O_2$) or presence of CBS (+1xBi, +2xBi and +5xBi). **f** Normalized CS reactivation for (**e**) at 100 s. Data are represented as mean of four replicates ± SEM. The *asterisks* indicated statistical significance (**$p \leq 0.01$)

constant (K_m), turnover number, k_{cat} and catalytic efficiency, k_{cat}/K_m were obtained via non-linear regression fitting of the titration data with Michaelis–Menten model (Tables S2, S3). Larger K_m values for Bi-AhpC towards the three ROS were found (Tables S2, S3), indicative of lower affinities of AhpC towards ROS substrates after Bi(III) treatment. Accordingly, the catalytic efficiencies (k_{cat}/K_m) decreased by half upon Bi(III) binding to AhpC, confirming the ability of Bi(III) in inhibiting antioxidant activity of AhpC towards simple inorganic hydroperoxide substrate, tertiary and bulky organic oxidative species (Tables S2, S3). Different from the simple peroxide species, lipid hydroperoxides bear greater cytotoxicity owing to the longer lifetime and higher mobility in migrating to subcellular organelles. Attenuation of the protective role of peroxiredoxins against oxidative species, especially lipid hydroperoxides, may increase lipid peroxidation, resulting in DNA damage and diminishing bacterial colonization in host [41, 42].

It has been demonstrated that the two conserved cysteines in peroxiredoxin family participate in the decomposition of ROS with the N-terminal cysteine being the peroxidatic residue to directly react with ROS; whereas the C-terminal cysteine being resolving cysteine for recycling the oxidized enzyme [43]. Such a differentiated reactivity of the two cysteine residues towards ROS has also been reported for AhpC [19]. We, therefore, investigated the effects of Bi(III) on enzymatic activity of the individual cysteine mutants of AhpC to examine the potential disparity of cysteine residues. The AhpC mutants AhpC-C49A and AhpC-C169A (pre-reduced by TCEP) were incubated with CBS for 15 min prior to FOX assay analysis. The activities of the untreated proteins were set at 100% for normalization. The overall inhibitory effects of CBS on both AhpC mutants against the three oxidants (each at 200 μM), i.e., H_2O_2, *t*-BuOOH and $PhC(CH_3)_2OOH$, are shown in Figures S2B and S1C. The inhibitory effect of CBS on AhpC-C49A was less pronounced than that on AhpC-C169A, suggesting that Bi(III) exerts greater effect on Cys49 than on Cys169.

Bi(III) drug interrupts chaperone activity of AhpC

It has been demonstrated previously that AhpC acts as a peroxide reductase to reduce organic hydroperoxides as well as a molecular chaperone to prevent protein misfolding under oxidative stress via shifting its molecular weight from low-molecular oligomers to high-molecular weight complex [20, 44]. The effects of Bi(III) (as CBS) on chaperone activity of AhpC was evaluated according to previous reports [29, 30]. AhpC pre-reduced by TCEP was incubated with or without (as a control) CBS prior to H_2O_2 treatment. Since it has been previously reported that the chaperone activity of AhpC was attributed to the hyperoxidation-induced shift to higher oligomeric state, presence of higher order oligomer of AhpC due to hyperoxidation was confirmed by native PAGE prior to chaperone activity assay (data not shown). These solutions were then mixed with denatured citrate synthase (dCS) and the ability of AhpC or Bi-AhpC to refold citrate synthase to its native state was examined by monitoring the decrease of UV absorbance at 233 nm owing to its interaction with acetyl-CoA. The UV absorbance at 500 nm attributable to improper refolding of citrate synthase was also monitored [29, 30]. As shown in Fig. 2d, e, mixing denatured citrate synthase with H_2O_2-treated Bi-AhpC led to much higher absorbance at 500 nm than that with H_2O_2-treated AhpC, indicative of higher degree aggregation of citrate synthase in the presence of H_2O_2-treated Bi-AhpC. This is in line with the enzymatic assay of citrate synthase (Fig. 2e), a less extent of restoration of functional citrate synthase manifested by the drop of UV absorbance at 233 nm was observed for H_2O_2-treated Bi-AhpC than H_2O_2-treated AhpC. Based on the normalized activities (Fig. 2f), in the presence of equimolar amounts of CBS, the chaperone activity of H_2O_2-treated AhpC dropped by about 40%, and further 20% reduction in its chaperon activity was observed in the presence of 5 molar equivalents of Bi(III), where ca. 20% of citrate synthase activity was re-stored (Fig. 2f), similar to the background of spontaneous self-refolding of denatured citrate synthase [29]. Thus, CBS abolishes the capability of AhpC on salvage of excessive unfolded proteins resulted from severe oxidative stress, which is likely to be lethal to the pathogen.

Inhibition of AhpC activities by Bi(III) reduces bacterial tolerance to oxidative stress and attenuates bacterial growth

To investigate the biological significance of functional disruption of AhpC by Bi(III), we attempted to delete *ahpC* gene from *H. pylori* by allelic exchange of *ahpC* gene on *H. pylori* chromosome with a kanamycin resistance gene [21]. However, no colonies were observed on selective agar plate under normal microaerophilic condition (data not shown), such a phenomenon was also observed previously [45], likely due to the fact that thioredoxin-dependent peroxiredoxin system, being the third most abundant protein expressed in *H. pylori*, is essential for the survival of bacterium [21]. Given that the peroxiredoxins were found in a diverse spectrum of microbial pathogens, e.g., *E. coli, M. tuberculosis* and *S. typhimurium*, we used *E. coli* as a model system to study the binding of CBS to AhpC on bacterial response towards oxidative stress. We first examined whether *ahpC* gene deletion influenced the bacterial survival under oxidation stress. Wild-type *E. coli* K12 strain BW25113 (WT) [31] with and without CBS treatment

and *ahpC* gene-deleted variant (KO) from KEIO collection [32] were subjected to 0–5 mM of *t*-BuOOH, followed by inoculation into fresh medium for overnight. The growth of the KO strain and CBS-treated wild-type *E. coli* (WT + Bi) were normalized against that of the untreated WT. As shown in Fig. 3a, the WT strain exhibited high tolerance against *t*-BuOOH at all concentrations tested, with over 80% growth recovery even in the presence of as high as 5 mM *t*-BuOOH. In contrast, Bi-treated WT showed a concentration-dependent decline in growth with only about 30% recovery upon exposure to 5 mM *t*-BuOOH; while the KO strain exhibits lower tolerance with ca. 25% recovery upon exposure of same amounts of *t*-BuOOH, treatment of the KO strain by CBS caused only subtle changes in the bacterial growth (Fig. 3a).

The bacterial growth for the WT, KO strains with and without CBS treatment under the stress of 5 mM *t*-BuOOH was also monitored at different time intervals. Under the condition used, the growth of WT was not perturbed by *t*-BuOOH or CBS alone as reflected by the similar cell density owing to its antioxidant defending system (Fig. 3b). In contrast, its growth was significantly retarded when treated with 50 μM CBS under the stress of 5 mM *t*-BuOOH (Fig. 3b). This indicates that Bi(III) might inhibit the activity of antioxidant enzymes including AhpC and reduce tolerance towards ROS as Bi(III) exhibits no antimicrobial activity against *E. coli*. Interestingly, the KO and Bi-treated KO strains exhibited a similar trend in defective growth upon exposure to 5 mM *t*-BuOOH (Fig. 3c), indicating that Bi(III) exerts negligible effect on *E. coli* growth once *ahpC* gene is deleted. Under the stress of 5 mM *t*-BuOOH, the activities of antioxidants in *E. coli* dropped with the addition of increasing amounts of Bi(III) and leveled off at 5 μM CBS, where ca. 40% activity was reduced (Fig. 3d). Similarly, deletion of *ahpC* in *E. coli* resulted in drop of the activity by ca. 50% (Fig. 3e). To further examine the role of AhpC in ROS tolerance in bacteria, *ahpC* gene was

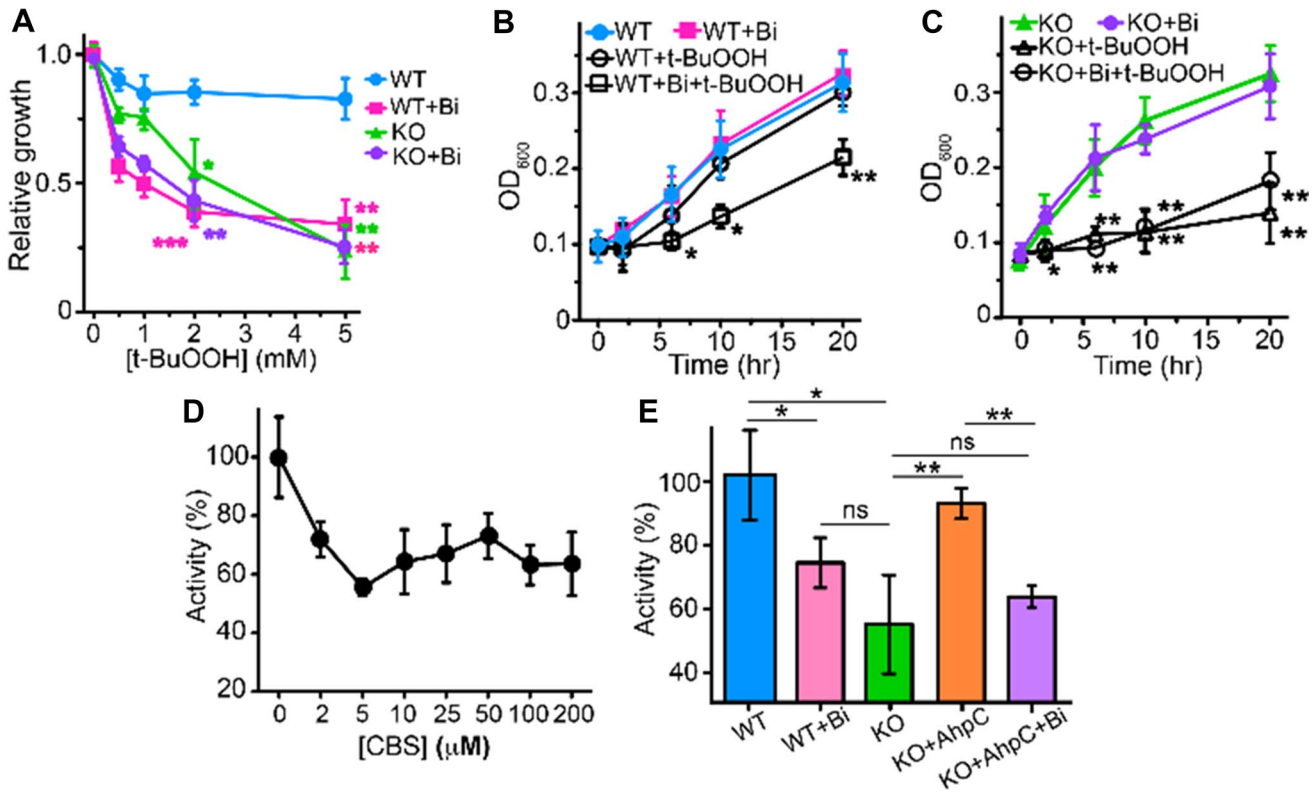

Fig. 3 Interaction of CBS with AhpC attenuates bacterial growth. **a** Relative growth of *E. coli* strain K12 (WT), Bi-treated (50 μM, WT + Bi), *ahpC* gene knocked out (KO) and bi-treated KO (50 μM, KO + Bi) strains after treatment with 0–5 mM of *tert*-butyl hydroperoxide (*t*-BuOOH). Time-dependent optical density at 600 nm (OD_{600}) for **b** WT or WT + Bi and **c** KO or KO + Bi with or without *t*-BuOOH treatment (5 mM). **d** Normalized activity of antioxidants in *E. coli* strain K12 against 5 mM *t*-BuOOH upon incubation with 0–200 μM of CBS. **e** Normalized activity of antioxidants in *E. coli* strain K12 (WT), Bi-treated (50 μM, WT + Bi), *ahpC* gene knockout (KO) strain, *ahpC*-complemented KO strain without (KO + AhpC) and with Bi(III) treatment (50 μM, KO + AhpC + Bi) against 5 mM *t*-BuOOH. Data are represented as mean of three replicates ± SEM. Statistical analysis in **a**–**c** were performed with reference to the respective untreated samples. The *asterisks* indicated statistical significance (*$P \leq 0.05$; **$P \leq 0.01$; ***$P \leq 0.001$; ns means non-significant)

complemented to the KO strain by transforming a plasmid expressing *Hp*AhpC protein. As shown in Fig. 3e, the activity of antioxidant in *ahpC*-complemented KO strain (KO + AhpC) recovered to ca. 90% of that for the WT. However, addition of Bi(III) to *ahpC*-complemented KO strain led to the activity dropped by ca. 40% (KO + AhpC + Bi), which is comparable to those of the WT + Bi and the KO strain (Fig. 3e). Taken together, we demonstrate that under oxidative stress, supplementation of CBS to the bacterial culture medium resulted in reduced bacterial growth and ROS tolerance, which is attributable to the inhibition of AhpC activity by Bi(III) and the role of AhpC might not be compensated by other ROS scavengers. It has been shown previously that the lethality of bactericidal antibiotics is enhanced by an increase in ROS level while deficiency in AhpC raised the sensitivity of bacteria towards ampicillin, kanamycin and norfloxacin [46]. Therefore, supplementation of Bi(III) drugs to bacterial culture medium is likely equivalent to "silencing" of *ahpC* gene in protein expression context.

To further examine the effects of bismuth drugs on AhpC antioxidant activity in *H. pylori*, *H. pylori* strain 26695 and clinical isolate strain A30651 were cultured with and without the supplementation of CBS, the antioxidant activity of AhpC against *t*-BuOOH in the cell lysate was evaluated by FOX assay [28]. As shown in Fig. 4, supplement of 10 μg/mL CBS to the culture medium of both *H. pylori* strains resulted in AhpC activity dropped by 25%. The activity was further reduced to 35 and 60% in strain 26695 and A30651, respectively, upon the addition of 20 μg/mL CBS, indicating that Bi(III) drugs are indeed able to disrupt the antioxidant activity of AhpC in the bacterium. Given the critical role of AhpC in *H. pylori* [20], we believe that functional disruption of AhpC by bismuth drugs might contribute significantly to the antimicrobial activity of bismuth drugs.

Bi(III) drugs restrains intracellular dynamic translocation of AhpC

AhpC was previously reported to be able to shuttle between membrane region and bacterial cytoplasm depending on its functions [20]. To investigate whether binding of Bi(III) to AhpC affects its intracellular dynamics, i.e., translocation, we employed a home-made fluorescent probe, Ni-*NTA-AC,* which can rapidly track intracellular His_6-tagged proteins in live cells [37], to monitor the intracellular localization of His_6-tagged AhpC in *E. coli* cells with *Hp*AhpC overexpression, whereas the membrane was marked by a BODIPY® lipid probe (BODIPY® 558/568 C12) [36, 37]. Upon supplement of 100 μM Ni-*NTA-AC* to the culture medium of His_6-tagged AhpC-overexpressing *E. coli* cells, blue fluorescence (excited at 356 nm and emitted at 448 nm) was observed in the cytoplasmic region of live *E. coli* (Fig. 5a), confirming that AhpC is mainly localized in the cytoplasm of the bacterium.

Upon addition of 2 mM *t*-BuOOH, intense blue fluorescence on the inner membrane was observed under identical conditions, roughly colocalized with the membrane probe BODIPY® (emitted at 569 nm) (Fig. 5c), indicative of translocation of AhpC from cytoplasm to the cell membrane under ROS stress, in agreement with a previous report that AhpC as a peroxide reductase is generally located on the bacterial membrane [23]. When the *E. coli* cells were treated with 50 μM Bi(III) (as CBS) prior to the addition of Ni-*NTA-AC* (100 μM), we observed blue fluorescence evenly distributed in cytosolic region of the bacterium (Fig. 5b). Surprisingly, exposure of the Bi(III)-treated *E. coli* cells to 2 mM *t*-BuOOH led to a fluorescence pattern similar to that of only Bi(III)-treated cells, but different from that of the Bi(III)-untreated group (Fig. 5c), implicating no translocation of AhpC to the membrane region

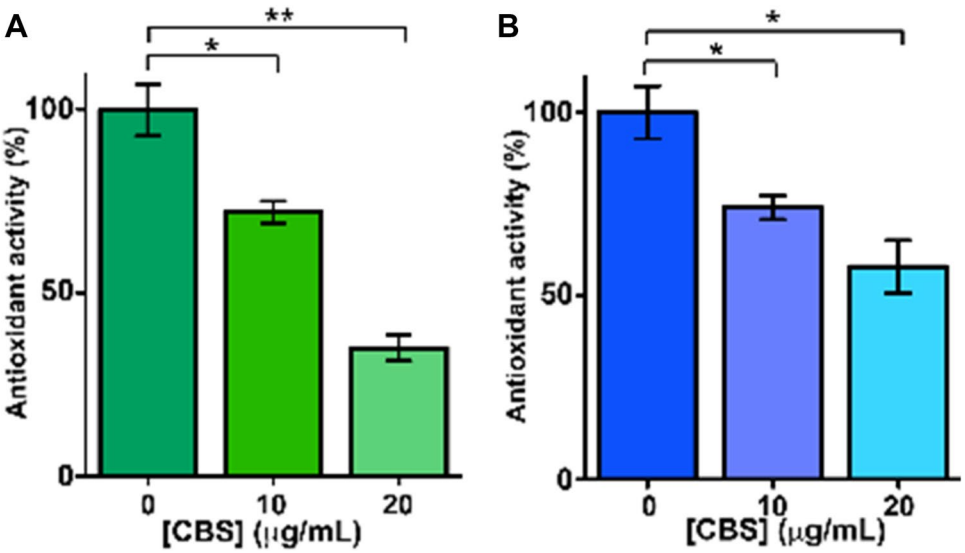

Fig. 4 Normalized antioxidant activity of AhpC in *H. pylori*. **a** Strain 26695 and **b** clinical isolate A30651. CBS with concentrations of 0, 10 and 20 μg/mL were supplemented in culture medium during bacterial growth and the antioxidant activities against *t*-BuOOH in the bacterial cell lysates were evaluated by FOX assay. Data are represented as mean of three replicates ± SEM. The *asterisks* indicated statistical significance (*$P \leq 0.05$; **$P \leq 0.01$)

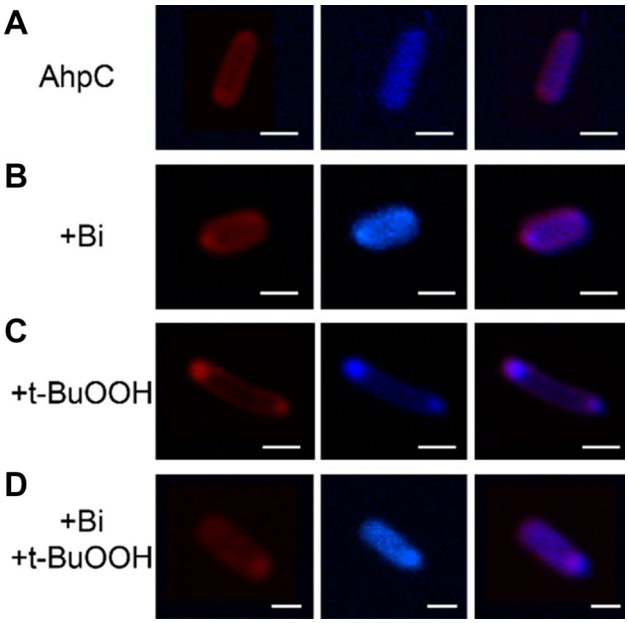

Fig. 5 Effect of CBS on dynamic translocation of AhpC in *E. coli* under oxidative stress. Confocal images of Ni–*NTA-AC*-labeled His_6-tagged AhpC in *Hp*AhpC-overexpressing *E. coli* cells **a** without or with addition of **b** CBS (50 μM) ($n = 5$) **c** 2 mM *t*-BuOOH **d** both CBS (50 μM) and 2 mM *t*-BuOOH ($n = 5$). The bacterial membrane was stained with a lipid probe BODIPY® 558/568 (*left*, *red*) while the His_6-tagged *Hp*AhpC was visualized using Ni–*NTA-AC* (100 μM) (*middle*, *blue*). Overlay of the images are shown in the *right panel* (*Scale bar* 1 μm)

upon exposure to ROS (Fig. 5d). Clearly, binding of Bi(III) to AhpC restrains the intracellular translocation of AhpC under oxidative stress, possibly due to the disturbance of oligomeric state of AhpC in bacteria.

Conclusions

We have demonstrated that Bi(III) binds to the conserved cysteine residues of AhpC, which serves as one of the essential peroxide reductases in *H. pylori*. Subsequent in vitro studies reveal that binding of Bi(III) to AhpC disrupts both its antioxidant and chaperone activities. Using *E. coli* as a model system, we show that deletion of *ahpC* gene led to a similar consequence as treatment of bismuth to the bacterium under oxidative stress, leading to significant attenuation of bacterial growth. Indeed, the antioxidant activity was reduced by bismuth drugs in *H. pylori*. Moreover, upon exposure to ROS, bismuth drugs perturb AhpC dynamic translocation between cytosolic and membrane region, which could be crucial for executing its biological functions. The multiple inhibitory effects of bismuth drugs on peroxiredoxins might result in interruption of various cellular processes, including oxidative defense, protecting proteins from misfolding under environmental stress and cellular signaling, which are necessary for the bacterial survival and pathogenesis [20, 47, 48]. Therefore, AhpC might serve as an important target for the development of antimicrobial agents.

Acknowledgements This work was supported by the Research Grants of Council of Hong Kong (703913, 17304614, 17305415, 17333616), Livzon Pharmaceutical Group, the University of Hong Kong (for an emerging Strategic Research Theme on Integrative Biology). We thank the assistance of Li Ka Shing Faculty of Medicine Faculty Core Facility, The University of Hong Kong. We thank Prof. Patrick Chiu Yat Woo (Department of Microbiology, LKS Faculty of Medicine) for his generous offer of clinical isolate of *H. pylori* strain. We thank Dr. Ligang Hu for his helpful comments and suggestions and Dr. Yau-Tsz Lai for suggestions on microscopic analysis.

References

1. Morones-Ramirez JR, Winkler JA, Spina CS, Collins JJ (2013) Silver enhances antibiotic activity against gram-negative bacteria. Sci Transl Med 5:190ra181
2. Dore MP, Lu H, Graham DY (2016) Role of bismuth in improving Helicobacter pylori eradication with triple therapy. Gut 65:870–878
3. Marshall BJ, Goodwin CS, Warren JR, Murray R, Blincow ED, Blackbourn SJ, Phillips M, Waters TE, Sanderson CR (1988) Prospective double-blind trial of duodenal ulcer relapse after eradication of *Campylobacter pylori*. Lancet 2:1437–1442
4. Fock KM, Graham DY, Malfertheiner P (2013) *Helicobacter pylori* research: historical insights and future directions. Nat Rev Gastroenterol Hepatol 10:495–500
5. Li H, Sun H (2012) Recent advances in bioinorganic chemistry of bismuth. Curr Opin Chem Biol 16:74–83
6. Polk DB, Peek RM Jr (2010) *Helicobacter pylori*: gastric cancer and beyond. Nat Rev Cancer 10:403–414
7. Yamaoka Y (2010) Mechanisms of disease: *Helicobacter pylori* virulence factors. Nat Rev Gastroenterol Hepatol 7:629–641
8. Megraud F (2012) The challenge of *Helicobacter pylori* resistance to antibiotics: the comeback of bismuth-based quadruple therapy. Ther Adv Gastroenterol 5:103–109
9. Malfertheiner P (2010) Infection—bismuth improves PPI-based triple therapy for *H. pylori* eradication. Nat Rev Gastroenterol Hepatol 7:538–539
10. Laine L, Hunt R, El-Zimaity H, Nguyen B, Osato M, Spenard J (2003) Bismuth-based quadruple therapy using a single capsule of bismuth biskalcitrate, metronidazole, and tetracycline given with omeprazole versus omeprazole, amoxicillin, and clarithromycin for eradication of *Helicobacter pylori* in duodenal ulcer patients: a prospective, randomized, multicenter, North American trial. Am J Gastroenterol 98:562–567
11. Cun S, Sun H (2010) A zinc-binding site by negative selection induces metallodrug susceptibility in an essential chaperonin. Proc Natl Acad Sci USA 107:4943–4948
12. Xia W, Li H, Sun H (2014) Functional disruption of HypB, a GTPase of *Helicobacter pylori*, by bismuth. Chem Commun 50:1611–1614
13. Cun SJ, Li HY, Ge RG, Lin MCM, Sun HZ (2008) A histidine-rich and cysteine-rich metal-binding domain at the C terminus of heat shock protein A from *Helicobacter pylori*—implication for nickel homeostasis and bismuth susceptibility. J Biol Chem 283:15142–15151

14. Ge R, Zhang Y, Sun X, Watt RM, He QY, Huang JD, Wilcox DE, Sun H (2006) Thermodynamic and kinetic aspects of metal binding to the histidine-rich protein, Hpn. J Am Chem Soc 128:11330–11331
15. Zhang L, Mulrooney SB, Leung AF, Zeng Y, Ko BB, Hausinger RP, Sun H (2006) Inhibition of urease by bismuth(III): implications for the mechanism of action of bismuth drugs. Biometals 19:503–511
16. Wang Y, Tsang CN, Xu F, Kong PW, Hu L, Wang J, Chu IK, Li H, Sun H (2015) Bio-coordination of bismuth in *Helicobacter pylori* revealed by immobilized metal affinity chromatography. Chem Commun 51:16479–16482
17. Ge R, Sun X, Gu Q, Watt RM, Tanner JA, Wong BC, Xia HH, Huang JD, He QY, Sun H (2007) A proteomic approach for the identification of bismuth-binding proteins in *Helicobacter pylori*. J Biol Inorg Chem 12:831–842
18. Stent A, Every AL, Sutton P (2012) *Helicobacter pylori* defense against oxidative attack. Am J Physiol Gastrointest Liver Physiol 302:G579–G587
19. Bryk R, Griffin P, Nathan C (2000) Peroxynitrite reductase activity of bacterial peroxiredoxins. Nature 407:211–215
20. Chuang M-H, Wu M-S, Lo W-L, Lin J-T, Wong C-H, Chiou S-H (2006) The antioxidant protein alkylhydroperoxide reductase of *Helicobacter pylori* switches from a peroxide reductase to a molecular chaperone function. Proc Natl Acad Sci USA 103:2552–2557
21. Baker LM, Raudonikiene A, Hoffman PS, Poole LB (2001) Essential thioredoxin-dependent peroxiredoxin system from *Helicobacter pylori*: genetic and kinetic characterization. J Bacteriol 183:1961–1973
22. Wang G, Olczak AA, Walton JP, Maier RJ (2005) Contribution of the *Helicobacter pylori* thiol peroxidase bacterioferritin comigratory protein to oxidative stress resistance and host colonization. Infect Immun 73:378–384
23. Huang CH, Chuang MH, Lo WL, Wu MS, Wu YH, Wu DC, Chiou SH (2011) Alkylhydroperoxide reductase of *Helicobacter pylori* as a biomarker for gastric patients with different pathological manifestations. Biochimie 93:1115–1123
24. Jang HH, Lee KO, Chi YH, Jung BG, Park SK, Park JH, Lee JR, Lee SS, Moon JC, Yun JW, Choi YO, Kim WY, Kang JS, Cheong GW, Yun DJ, Rhee SG, Cho MJ, Lee SY (2004) Two enzymes in one; two yeast peroxiredoxins display oxidative stress-dependent switching from a peroxidase to a molecular chaperone function. Cell 117:625–635
25. Moon JC, Hah YS, Kim WY, Jung BG, Jang HH, Lee JR, Kim SY, Lee YM, Jeon MG, Kim CW, Cho MJ, Lee SY (2005) Oxidative stress-dependent structural and functional switching of a human 2-Cys peroxiredoxin isotype II that enhances HeLa cell resistance to H_2O_2-induced cell death. J Biol Chem 280:28775–28784
26. Hu L, Cheng T, He B, Li L, Wang Y, Lai Y-T, Jiang G, Sun H (2013) Identification of metal-associated proteins in cells by using continuous-flow gel electrophoresis and inductively coupled plasma mass spectrometry. Angew Chem Intl Ed 52:4916–4920
27. Bai YC, Wu FC, Liu CQ, Li W, Guo JY, Fu PQ, Xing BS, Zheng J (2008) Ultraviolet absorbance titration for determining stability constants of humic substances with Cu(II) and Hg(II). Anal Chim Acta 616:115–121
28. Nelson KJ, Parsonage D (2011) Measurement of peroxiredoxin activity. Curr Protoc Toxicol 49:7.10.1–7.10.28
29. Steede NK, Temkin SL, Landry SJ (2000) Assay of chaperonin-assisted refolding of citrate synthase. In: Schneider C (ed) Chaperonin protocols 2001/08/04 edn. Humana Press Inc., Totowa, pp 133–138
30. Wiech H, Buchner J, Zimmermann R, Jakob U (1992) Hsp90 chaperones protein *folding in vitro*. Nature 358:169–170
31. Datsenko KA, Wanner BL (2000) One-step inactivation of chromosomal genes in *Escherichia coli* K-12 using PCR products. Proc Natl Acad Sci USA 97:6640–6645
32. Baba T, Ara T, Hasegawa M, Takai Y, Okumura Y, Baba M, Datsenko KA, Tomita M, Wanner BL, Mori H (2006) Construction of *Escherichia coli* K-12 in-frame, single-gene knockout mutants: the Keio collection. Mol Syst Biol 2(2006):0008
33. Menard R, Sansonetti PJ, Parsot C (1993) Nonpolar mutagenesis of the ipa genes defines IpaB, IpaC, and IpaD as effectors of *Shigella flexneri* entry into epithelial cells. J Bacteriol 175:5899–5906
34. Carpenter BM, McDaniel TK, Whitmire JM, Gancz H, Guidotti S, Censini S, Merrell DS (2007) Expanding the *Helicobacter pylori* genetic toolbox: modification of an endogenous plasmid for use as a transcriptional reporter and complementation vector. App Environ Microbiol 73:7506–7514
35. Ge Z, Taylor DE (1997) *H. pylori* DNA transformation by natural competence and electroporation. In: Clayton CL, Mobley HLT (eds) *Helicobacter pylori* protocols. Humana Press, Totowa, pp 145–152
36. Chung KCC, Zamble DB (2011) Protein interactions and localization of the *Escherichia coli* accessory protein HypA during nickel insertion to [NiFe] hydrogenase. J Biol Chem 286:43081–43090
37. Lai Y-T, Chang Y-Y, Hu L, Yang Y, Chao A, Du Z-Y, Tanner JA, Chye M-L, Qian C, Ng K-M, Li H, Sun H (2015) Rapid labeling of intracellular His-tagged proteins in living cells. Proc Natl Acad Sci USA 12:2948–2953
38. Sun H, Li H, Harvey I, Sadler PJ (1999) Interactions of bismuth complexes with metallothionein(II). J Biol Chem 274:29094–29101
39. Ge R, Sun H (2007) Bioinorganic chemistry of bismuth and antimony: target sites of metallodrugs. Acc Chem Res 40:267–274
40. Parsonage D, Karplus PA, Poole LB (2008) Substrate specificity and redox potential of AhpC, a bacterial peroxiredoxin. Proc Natl Acad Sci USA 105:8209–8214
41. Dwyer DJ, Kohanski MA, Collins JJ (2009) Role of reactive oxygen species in antibiotic action and resistance. Curr Opin Microbiol 12:482–489
42. Wang G, Hong Y, Johnson MK, Maier RJ (2006) Lipid peroxidation as a source of oxidative damage in *Helicobacter pylori*: protective roles of peroxiredoxins. Biochim Biophys Acta 1760:1596–1603
43. Wood ZA, Schroder E, Robin Harris J, Poole LB (2003) Structure, mechanism and regulation of peroxiredoxins. Trends Biochem Sci 28:32–40
44. An BC, Lee SS, Lee EM, Lee JT, Wi SG, Jung HS, Park W, Chung BY (2010) A new antioxidant with dual functions as a peroxidase and chaperone in *Pseudomonas aeruginosa*. Mol Cells 29:145–151
45. Lundstrom AM, Bolin I (2000) A 26 kDa protein of *Helicobacter pylori* shows alkyl hydroperoxide reductase (AhpC) activity and the mono-cistronic transcription of the gene is affected by pH. Microb Pathog 29:257–266
46. Dwyer DJ, Belenky PA, Yang JH, MacDonald IC, Martell JD, Takahashi N, Chan CTY, Lobritz MA, Braff D, Schwarz EG, Ye JD, Pati M, Vercruysse M, Ralifo PS, Allison KR, Khalil AS, Ting AY, Walker GC, Collins JJ (2014) Antibiotics induce redox-related physiological alterations as part of their lethality. Proc Natl Acad Sci USA 111:E2100–E2109
47. Sobotta MC, Liou W, Stöcker S, Talwar D, Oehler M, Ruppert T, Scharf AN, Dick TP (2015) Peroxiredoxin-2 and STAT3 form a redox relay for H_2O_2 signaling. Nat Chem Biol 11:64–70
48. Teixeira F, Castro H, Cruz T, Tse E, Koldewey P, Southworth DR, Tomás AM, Jakob U (2015) Mitochondrial peroxiredoxin functions as crucial chaperone reservoir in *Leishmania infantum*. Proc Natl Acad Sci USA 112:E616–E624